

Enhanced Adsorption Property of TiO₂ Based Nanoribbons Produced by Alkaline Hydrothermal Process

Dessy Ariyanti^{1,2*}, Satriani Mo'ungatonga², Wei Gao²

¹Department of Chemical Engineering, Faculty of Engineering, Universitas Diponegoro
Jl. Prof. H. Soedarto, SH., Tembalang, Semarang, 50275, Indonesia

²Department of Chemical & Materials Engineering, Faculty of Engineering, University of Auckland
Auckland 1142, New Zealand

Abstract

TiO₂ is a semiconductor material with endless potential for the development of renewable energy as well as in the environmental field application. With various methods, TiO₂ nanostructures with various morphology, properties and application can be developed. In this paper, the synthesis of TiO₂ based nanoribbons with high adsorption property produced by alkaline hydrothermal methods were investigated. Its morphology, crystal structure and physical properties were characterized using Scanning Electron Microscope (SEM), X-ray diffraction (XRD), Fourier-transform infrared (FTIR) and Brunauer-Emmett-Teller (BET) surface area analysis. The result shows that by controlling the hydrothermal processing time, different morphology and structures of TiO₂ nanoribbons with different adsorption properties can be obtained. The nanoribbons produced via alkaline hydrothermal method has width 200-300 nm and length up to several microns. It also possesses fair adsorption capacity over dyes (Rhodamine B and Methyl orange) considering its large surface area and high pore volume.

Keywords: Nanoribbon, nanowires, TiO₂ hydrogen trititanate, adsorption, Rhodamine

INTRODUCTION

TiO₂ based nanostructures has unique physicochemical properties and morphology which can be used for many applications such as catalysis, gas adsorption (Umek *et al.*, 2005), in lithium battery (Kavan *et al.*, 2004; Myung *et al.*, 2011) and solar cells (Pan *et al.*, 2007). Morphology such as nanotubes, nanoribbons, nanobelts, nanorods, and nanowires may form during the process depending on the process parameters. Kasuga *et al.* were first reported the method namely alkaline hydrothermal in 1998 to produced TiO₂ based nanostructures. This method was able to convert amorphous TiO₂ into nanotubes and nanoribbons with almost 100% efficiency Kasuga *et al.*, 2005; Bavykin *et al.*, 2006). The application of TiO₂ nanoribbon varied such as the photocatalyst nanohybrid with carbon nanotubes for water splitting photoelectrochemical (PEC) enhancement (Ahmed *et al.*, 2020); anode material in combination with SnO₂ for

rechargeable battery (Li *et al.*, 2016); organic pollutant removal (Ariyanti *et al.*, 2018 Ariyanti *et al.*, 2019).

Researchers reported low adsorption properties of TiO₂ based nanoribbons, which has a typical value of specific surface area in the range of 20–25 m²/g and pore volume below 0.1 cm³/g (Umek *et al.*, 2005; Bavykin *et al.*, 2006). In this study, the investigation on TiO₂ based nanoribbons with high adsorption property using alkaline hydrothermal methods were conducted. The reaction mechanisms that lead to the formation of different types of layered protonated titanate are also discussed. In addition, the ability of layered protonated titanate on dye adsorption is correlated with its morphology and crystal phases.

METHODOLOGY

The starting material for this experiment was TiO₂ powder anatase phase with particle size

<25nm (purchased from Sigma Aldrich Co.). The synthesis of TiO₂ based nanostructure via alkaline hydrothermal method was initiated by the dispersion of 0.2 g anatase powder in the 30mL 10M NaOH solution with continuous mixing to achieve the homogenized solution. The well mixed solution then transferred immediately to a hydrothermal autoclave equipped with Teflon-lined, sealed properly for safety purposes and placed in an oven at 180°C for 15-30h. The products after it cooled down then firstly washed with 0.1M HCl, followed by deionized water, and then dried in the oven at 120°C for 4h.

Samples was first characterized by Scanning Electron Microscope with (SEM-EDS, Philips XL30S FEG) to observed the morphology of the nanostructures. The X-ray diffraction (XRD) was used to analyze its crystal structures and FTIR (Perkin Elmer FT-IR Spectroscopy ATR) was employed to investigate the chemical bonding of the samples. In addition the Brunauer–Emmett–Teller (BET) total surface area was evaluated using TriStar 3000 surface area analyser along with the average pore diameter using Barrett–Joyner–Halenda (BJH) method and the cumulative pore volume.

Batch experiment was conducted to evaluated the adsorption capacity of the samples over dyes. Representative dyes such as Rhodamine B (RhB) and Methyl Orange (MO) with purity ≥ 95% and 85% respectively were purchased from Sigma Aldrich Co and used without prior treatment. 50 mg of nanoribbons sample was dispersed and mixed in 50 mL RhB or MO solution with concentration of 5ppm for 120 min. Every period of time 2 mL of sample was taken and then filtered with 0.2µm PVDF syringe filter for further concentration measurement. The concentrations of RhB and MO were determined by the adsorbance measurement at the at 553 nm for RhB and 463 nm for MO in UV-Vis spectrophotometer (Perkin Elmer).

RESULTS AND DISCUSSION

The alkaline hydrothermal reaction is a straightforward process initiated by mixing the as purchased TiO₂ with 10 M NaOH to form a well dispersed solution followed by heat treatment through hydrothermal process at 180°C. The

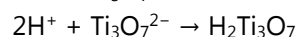
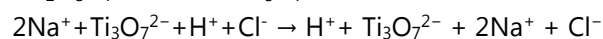
afterwards HCl treatment yields the TiO₂ based nanostructures. Figure 1 show the morphology of TiO₂ based nanostructure prepared at different times in comparison with the untreated TiO₂. Irregular thick nanoribbons were produced after 15 h of hydrothermal reaction (Figure 1B). Based on this SEM images it observed that the width of this nanoribbons range of 50-400 nm with up to several microns in length. Meanwhile, by setting up hydrothermal process for 20 h, thin ordered nanoribbons were produced (Figure 1C) with width observed in the range of 200-300 nm and several microns in length. Further, by prolonging the process time up to 30 h regular nanowires were produced with width of 50-100 nm and length of several microns (Figure 1D).

Figure 2 shows the XRD analysis of the nanoribbons prepared at 15 and 20 h. The structure was proven to be a monoclinic of hydrogen trititanate (H₂Ti₃O₇) with peaks at 11, 24.5, 33, and 48.4° (JCPDS 47-0561). The nanowires produced from hydrothermal process for 30 h appeared to be a mixture of H₂Ti₃O₇ (JCPDS 47-0561), B-TiO₂ (JCPDS 46-1238) and H₂Ti₅O₁₁·H₂O (JCPDS 44-0131). According to some researches, by taking the route of hydrothermal process, there are several possibilities of structures may be produced with mostly layered protonated titanates such as H₂Ti₃O₇, H₂Ti₂O₄(OH)₂, H₂Ti₄O₉·H₂O, TiO₂-B or H₂Ti₅O₁₁·H₂O. Thus are depending on the parameters such as temperature and operation time used during alkaline hydrothermal treatment and the acid washing treatment (Bavykin *et al.*, 2006; Gao *et al.*, 2013).

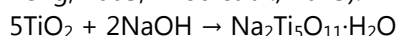
In general, there are two reaction steps in sequence during the hydrothermal process, (i) formation of layered titanate and (ii) dissolution followed by re-crystallisation along with the ion exchange. The chemical reactions are suggested below (Gao *et al.*, 2013; Lai *et al.*, 2015):

TiO₂ dissolved in 10 M NaOH solution for 15-20 h:
 $3\text{TiO}_2 + 2\text{NaOH} \rightarrow \text{Na}_2\text{Ti}_3\text{O}_7 + \text{H}_2\text{O}$

Washing with HCl for 24 h:



Above 24 h hydrothermal process, sodium pentatitanate formed via the reactions listed (Yang and Zeng, 2005; Zhou *et al.*, 2015):



Washing with HCl for 24 h:



The formation of B-TiO₂ with 30 h hydrothermal treatment is due to H₂Ti₃O₇ reorganization as a result of heat treatment and continuous water loss (Ariyanti *et al.*, 2018; Zhu *et al.*, 2001).

Figure 3 shows the FT-IR spectra of TiO₂ based nanostructures prepared at variable of times. The peaks situated at 443 cm⁻¹ for all samples, corresponding to the Ti–O–Ti vibrational frequency. Meanwhile, Ti–O stretching vibrations of hydrogen titanates were also detected in vibration mode at 908 cm⁻¹ (Bavykin *et al.*, 2006), which only found in the samples prepared at 20 and 30 h. Furthermore, in all samples, at 3210 cm⁻¹

the broad spectrums were observed indicating the presence of –OH groups in the surface, and strong absorption at 1633 cm⁻¹ were also found which attributes to the deformation vibration of H–O–H bonds in the physically absorbed water. Another, IR absorption in the range of 1600–3600 cm⁻¹ detected indicates the manifestation of –OH groups and H–O–H molecules that are weakly bounded in different active sites of TiO₂ (Li *et al.*, 2005; Shankar *et al.*, 2009; Choudhury *et al.*, 2012; Ariyanti *et al.*, 2018).

Adsorption characterisation of TiO₂ based nanostructures prepared at different times were determined using N₂ adsorption at 77.35 K with a relative pressure (P/P₀) range of 0.0001 to 1 (Figure 4). Nanoribbons prepared using hydrothermal process for 20 h shows high adsorption of nitrogen. The BET and pore size distribution are shown in Table 1, confirming that the nanoribbons prepared at 20 h of hydrothermal process has a large surface area (89.805 m²/g) and high pore volume (0.384 cm³/g).

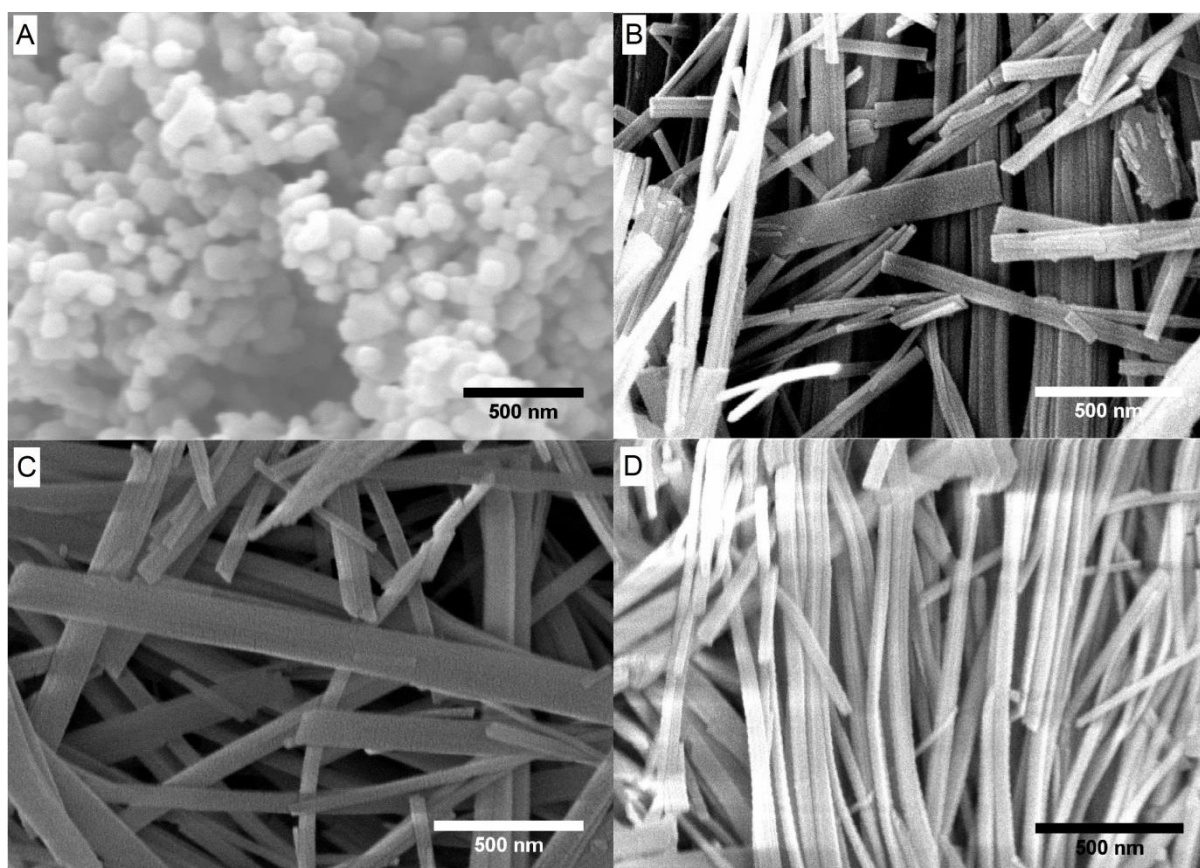


Figure 1. The SEM images of TiO₂ based nanostructures: (A) untreated TiO₂, (B) hydrothermally treated sample for 15 h, (C) 20 h, and (D) 30 h.

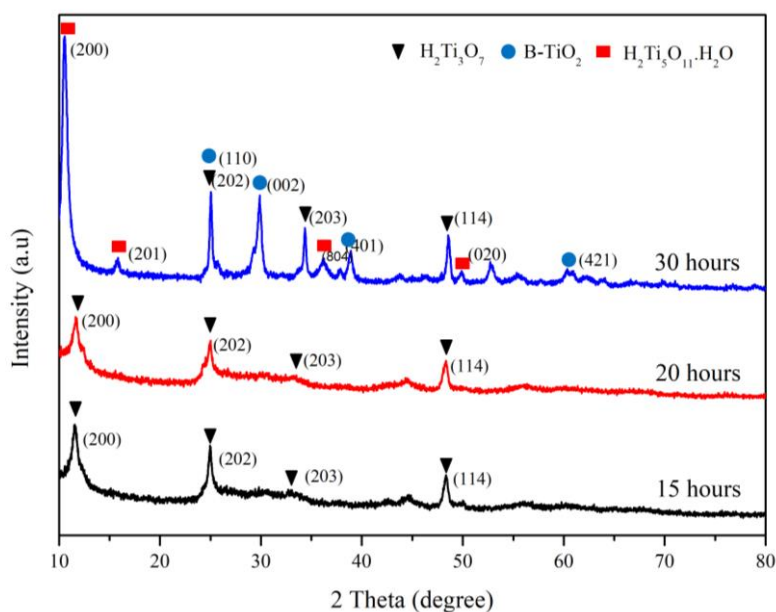


Figure 2. XRD patterns of TiO₂ based nanostructures prepared at different variable of times

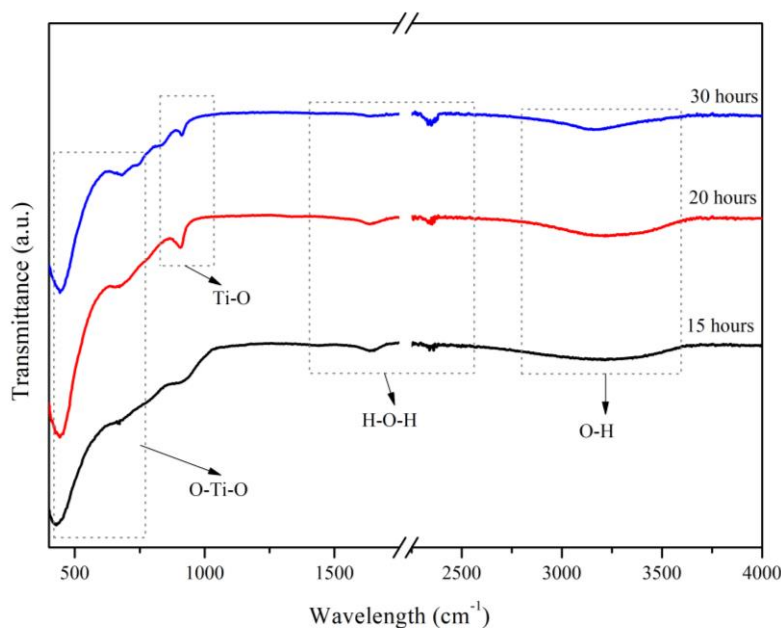


Figure 3. FT-IR spectra of TiO₂ based nanostructures prepared at variable of times

Adsorption capacity of TiO₂ based nanostructures prepared at different time was evaluated over adsorption of Rhodamine B and Methyl orange. As depicted in Figure 5, nanoribbons prepared with hydrothermal process for 20 h possess higher adsorption capacity compared to the other samples. Adsorption capacity is largely decided by pore size and volume of adsorbent (Hsieh, and Teng, 2000;

Dąbrowski, 2001). Even though the nanoribbons (20h) have relatively small pore size, it still has higher pore volume compared to samples of 15h and 30h (3 times higher). The high BET surface area is favourable for the dye adsorption process.

It also observed that TiO₂ based nanostructures absorbed more concentration of Rhodamine B compared to Methyl Orange.

Rhodamine B and Methyl Orange are two different dyes, and it may have a considerable effect on the adsorption. Methyl orange is an azo group with (-N=N-) and sulfonic group on the other side. These

types of bonding are associated with high dissociation energy and less reactive (Horikoshi *et al.*, 2003; Luan *et al.*, 2013) compared to the functional groups existing in Rhodamine B.

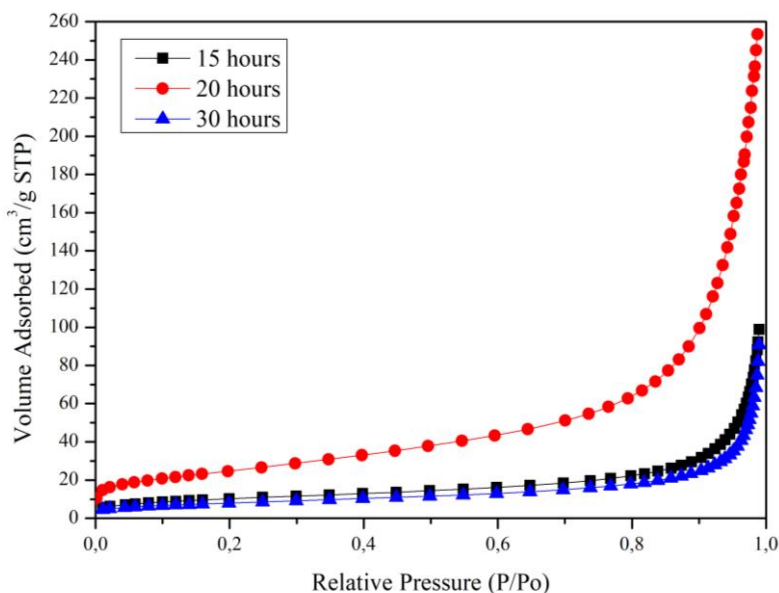


Figure 4. Nitrogen adsorption isotherms of TiO₂ based nanostructures prepared at different times

Table 1. Surface area and pore size distribution of TiO₂ based nanostructures prepared at various times

Samples	S _{BET} (m ² /g)	Pore volume (cm ³ /g)	Pore size (nm)
15 h	37.743	0.148	18.437
20 h	89.805	0.384	15.896
30 h	29.240	0.138	19.825

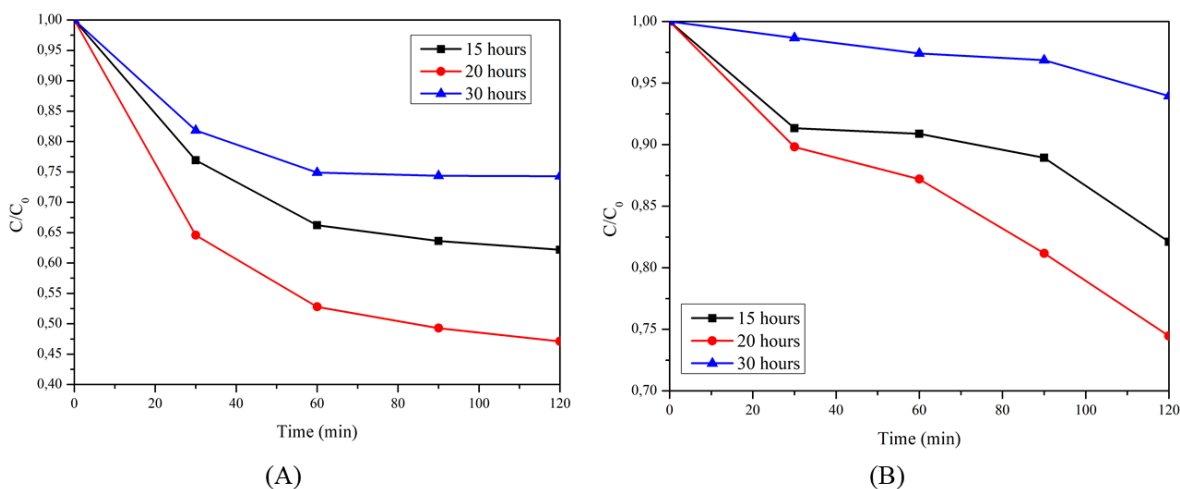


Figure 5. Adsorption capacity of TiO₂ based nanostructures prepared at different times for: (A) Rhodamine B, and (B) Methyl orange

CONCLUSION

The formation of TiO₂ based nanostructures by alkaline hydrothermal technique has been investigated at different processing times. By controlling the processing time, different morphologies and structures can be obtained. Different processing times could lead to different reaction mechanisms that associated with different crystal structures. Furthermore, variation of TiO₂ based nanostructures obtained from the alkaline hydrothermal process also decides the adsorption properties. Nanoribbons with width 200-300 nm and length up to several microns possesses fair adsorption capacity over dyes such as Rhodamine B and Methyl orange with their respective adsorption capacity considering its large surface area and high pore volume.

REFERENCES

- Umek, P., Cevc, P., Jesih, A., Gloter, A., Ewels, C.P. & Arçon, D., 2005. Impact of structure and morphology on gas adsorption of titanate-based nanotubes and nanoribbons. *Chemistry of materials*, 17(24):5945-5950.
- Kavan, L., Kalbác, M., Zúkalová, M., Exnar, I., Lorenzen, V., Nesper, R. & Graetzel, M., 2004. Lithium storage in nanostructured TiO₂ made by hydrothermal growth. *Chemistry of Materials*, 16(3):477-485.
- Myung, S.T., Takahashi, N., Komaba, S., Yoon, C.S., Sun, Y.K., Amine, K. & Yashiro, H., 2011. Nanostructured TiO₂ and Its Application in Lithium-Ion Storage. *Advanced Functional Materials*, 21(17):3231-3241.
- Pan, K., Zhang, Q., Wang, Q., Liu, Z., Wang, D., Li, J. & Bai, Y., 2007. The photoelectrochemical properties of dye-sensitized solar cells made with TiO₂ nanoribbons and nanorods. *Thin Solid Films*, 515(7-8):4085-4091.
- Kasuga, T., Hiramatsu, M., Hoson, A., Sekino, T. & Niihara, K. 1998. Formation of titanium oxide nanotube" *Langmuir*, 14(12):3160-3163.
- Bavykin, D. Friedrich, J. & Walsh, F. 2006. Protonated titanates and TiO₂ nanostructured materials: Synthesis, properties, and applications. *Advanced Materials*, 18(21):2807-2824.
- Ahmed, A.M., Mohamed, F., Ashraf, A.M., Shaban, M., Aslam Parwaz Khan, A. & Asiri, A.M. 2020. Enhanced photoelectrochemical water splitting activity of carbon nanotubes@TiO₂ nanoribbons in different electrolytes *Chemosphere*, 238:124554.
- Li, X., Zhang, X., Wang, R., Su, Z., Sha, J. & Liu, P. 2016. Graphene nanoribbons wrapping double nanoshells of SnO₂@TiO₂ for high lithium storage. *Journal of Power Sources*, 336:298-306.
- Ariyanti, D., Mo'ungatonga, S., Li, Y. & Gao, W. 2018. Formation of TiO₂ based nanoribbons and the effect of post-annealing on its photocatalytic activity. *IOP Conference Series: Materials Science and Engineering*, 348:012002.
- Ariyanti, D., Dong, J. & Gao, W. 2019. Hierarchical structures of coated TiO₂ nanoribbons with photodegradation and sedimentation properties. *International Journal of Modern Physics B*, 33(1n03):1940022.
- Gao, P., Bao, D., Wang, Y., Chen, Y., Wang, L., Yang, S., Chen, G., Li, G., Sun, Y. & Qin, W., 2013. Epitaxial growth route to crystalline TiO₂ nanobelts with optimizable electrochemical performance. *ACS Applied Materials & Interfaces*, 5(2):368-373.
- Lai, C.W., Bee Abd Hamid, S., Tan, T.L. & Lee, W.H. 2015. Rapid formation of 1D titanate nanotubes using alkaline hydrothermal treatment and its photocatalytic performance. *Journal of Nanomaterials*, 2015: e145360.
- Yang, H. G. & Zeng, H. C. 2005. Synthetic architectures of TiO₂/ H₂Ti₅O₁₁·H₂O, ZnO/H₂Ti₅O₁₁·H₂O, ZnO/ TiO₂/H₂Ti₅O₁₁·H₂O, and ZnO/TiO₂ nanocomposites. *Journal of the American Chemical Society*, 127(1):270-278.
- Zhou, R., Wei, D., Ke, H., Cao, J., Li, B., Cheng, S., Feng, W., Wang, Y., Jia, D. & Zhou, Y., 2015. H₂Ti₅O₁₁·H₂O nanorod arrays formed on a Ti surface via a hybrid technique of microarc oxidation and chemical treatment. *CrystEngComm*, 17(13):2705-2717.
- Zhu, G., Wang, C. & Xia, Y. 2011. Structural transformation of layered hydrogen trititanate (H₂Ti₃O₇) to TiO₂(B) and its electrochemical profile for lithium-ion intercalation. *Journal of Power Sources*, 196(5):2848-2853.

- Li, G., Li, L., Boerio-Goates, J. & Woodfield, B.F. 2005. High purity anatase TiO₂ nanocrystals: Near room-temperature synthesis, grain growth kinetics, and surface hydration chemistry. *Journal of the American Chemical Society*, 127(24):8659-8666.
- Shankar, K., Basham, J.I., Allam, N.K., Varghese, O.K., Mor, G.K., Feng, X., Paulose, M., Seabold, J.A., Choi, K.S. & Grimes, C.A., 2009. Recent advances in the use of TiO₂ nanotube and nanowire arrays for oxidative photoelectrochemistry. *The Journal of Physical Chemistry C*, 113(16):6327-6359.
- Choudhury, B., Borah, B. & Choudhury, A. 2012. Extending photocatalytic activity of TiO₂ nanoparticles to visible region of illumination by doping of cerium. *Photochemistry and photobiology*, 88(2):257-264. 2012.
- Hsieh, C. & Teng, H. 2000. Influence of mesopore volume and adsorbate size on adsorption capacities of activated carbons in aqueous solutions. *Carbon*, 38(6):863-869.
- Dąbrowski, 2001. Adsorption from theory to practice. *Advances in Colloid and Interface Science* 93(1-3):135-224.
- Horikoshi, S., Saitou, A., Hidaka, H. & Serpone, N. 2003. Environmental remediation by an integrated microwave/UV illumination method. V. thermal and nonthermal effects of microwave radiation on the photocatalyst and on the photodegradation of rhodamine-B under UV/vis radiation. *Environmental science & technology*, 37(24):5813-5822.
- Luan, J & Xu Y. 2013. Photophysical property and photocatalytic activity of new Gd₂InSbO₇ and Gd₂FeSbO₇ compounds under visible light irradiation. *International Journal of Molecular Sciences*, 14(1):999-1021